Polymer 49 (2008) 2298–2305

Contents lists available at ScienceDirect

Polymer

journal homepage: www.elsevier.com/locate/polymer

# Structure of segmented poly(ether urethane)s containing amino and hydroxyl functionalized polyhedral oligomeric silsesquioxanes (POSS)

V.N. Bliznyuk [a,*], T.A. Tereshchenko [b], M.A. Gumenna [b], Yu P. Gomza [b],
A.V. Shevchuk [b], N.S. Klimenko [b], V.V. Shevchenko [b,**]

[a] Department of Paper Engineering, Chemical Engineering and Imaging, Western Michigan University, Kalamazoo, MI 49008 5462, USA
[b] Institute of Macromolecular Chemistry of National Academy of Sciences of Ukraine, 48, Kharkivske shose, 02160 Kiev, Ukraine

ARTICLE INFO

*Article history:*
Received 6 December 2007
Received in revised form 19 February 2008
Accepted 23 February 2008
Available online 2 March 2008

*Keywords:*
Polyhedral oligomeric silsesquioxanes (POSS)
Polyurethane
Structure

ABSTRACT

Polyhedral oligomeric silsesquioxanes (POSS) with an empirical formula $[RSiO_{1.5}]_n$ (where $n = 6, 8, \ldots 14$, and R is a reactive organic group) represent a new type of nanomodifiers for polyurethanes (PUs) to produce organic–inorganic hybrids (OIHs), which are promising candidates for modern applications spreading from biomedical to airspace technologies. In this paper we report on the synthesis and structural organization of two different series of PU–POSS copolymers (branched and cross-linked) based on a mixture of variable size oligomeric silsesquioxanes (POSS-M) of a general formula $[(HOCH_2\text{-}CH(OH)CH_2)_2N(CH_2)_3SiO_{1.5}]_n$. Chemical structure of the synthesized POSS-M containing PUs has been confirmed by gel permeation chromatography and IR spectroscopic studies. Complex several-level hierarchy of their physical structural organization could be recognized from small angle X-ray scattering (SAXS) and atomic force microscopic (AFM) studies. SAXS experiments revealed that processes of microphase segregation and formation of nano-sized domains enriched with the inorganic phase (POSS fragments) take place during synthesis of the OIH systems. These nano-heterogeneity regions contain up to 66 vol.% of $SiO_{1.5}$ and form a paracrystalline lattice with hexagonal symmetry and characteristic interplanar periodicity of around 15 nm. The average size of inorganic phase nano-inclusions can be estimated as 2–3 nm, which corresponds to several POSS moieties in size. Cross-linked POSS-M containing PUs, as topologically more complex systems, is characterized with a diffusion-limited microphase segregation features. In the latter case the regions of nano-heterogeneity are smaller in size, have smaller content of the inorganic phase (ca. 54 vol.%), and form a less perfect paracrystalline order with the periodicity of 9.7 nm. Generally, we demonstrate that replacement of regular POSS moieties with the mixed POSS-M ones can lead to nanocomposite systems with an ordered supramolecular structural organization and simultaneous reduction of their production cost due to relative simplicity of their synthesis.

## 1. Introduction

Being constituted with two thermodynamically incompatible soft and hard blocks, segmented polyurethanes (PUs) are characterized with a unique combination of mechanical and thermal properties [1,2]. Variation of the chemical nature of one of the segments or both is a powerful tool of the structural control of these polymer materials' structure and properties. Such peculiarities of the segmented PU can be helpful in the creation of nanostructured organic–inorganic hybrid (OIH) materials [3]. Within the latter class of materials increasing interest lies in the usage of functional polyhedral oligomeric silsesquioxanes (POSS) with a general formula $(RSiO_{1.5})_n$ having natural silica-type nanoparticles with a well defined structure and topology as an inorganic phase [4]. These compounds possess partially or completely condensed silsesquioxane frame $[SiO_{1.5}]_n$ ($n = 6, 8, 10, \ldots$) having the same or different peripheral substitutes R, which may also include functional groups allowing further chemical reactions.

Development of the methods of inclusion of the POSS fragments into compositions of different polymers is mainly limited by the availability of new ways of a controlled “bottom–up” synthesis of nanostructured functional materials. The most widely used fragments (including segmented PUs) are individual compounds so-called octahedral POSS ($n = 8$) with the particle size of 1–3 nm containing 1–8 reactive groups [5–16]. Synthesis of amphiphilic telechelic oligourethanes with terminal POSS groups through reaction of monoisocyanate substituted POSS and oligo(oxyethylene diol) and investigation of the structure of such polymers in

---

* Corresponding author.
** Corresponding author.
*E-mail addresses:* valery.bliznyuk@wmich.edu (V.N. Bliznyuk), olga-s@mail.kar.net (V.V. Shevchenko).

0032-3861/$ – see front matter © 2008 Elsevier Ltd. All rights reserved.
doi:10.1016/j.polymer.2008.02.044

solution have been reported recently [5,6]. Interestingly, chemical reaction of monoisocyanate substituted POSS fragments with polyamidoamine of a dendritic nature (polyamidoamine PAMAM dendrimers) leads to the formation of several organo-inorganic core–shell type nano-hybrids [7]. Application of dihydroxy-containing POSS with isocyanate pre-polymers can yield linear segmented PUs with POSS fragments as a side group of the hard segments [8–12]. By analogy with this method diamino-POSS has been used to prepare nanostructured PU–POSS hybrid aqueous dispersions [13]. As demonstrated, reaction of the silanol groups of an open cage POSS with isocyanate moieties gave segmented PUs with POSS incorporated in the polymer main chain as a part of the hard segment [14]. Cross-linked PUs could be also synthesized through the reaction of octafunctional POSS with either isocyanate [15] or amine groups [16]. All these studies demonstrated that incorporation of POSS had a drastic effect on the structure and physical properties of segmented oligo- and polyurethane.

Unfortunately, all methods of chemical synthesis of the above mentioned reactive POSS moieties are characterized with relatively low yield of the final product and require a large number of stages, which increase the production cost and limit practical outcomes and prospects for commercialization of these potentially attractive materials. One of the possible ways to overcome the problem may be the application of a mixture of reactive POSS moieties instead of the monodisperse ones. In particular, hydrolytic condensation of a product of interaction of glycidol and 3-aminopropyl-triethoxysilane yields a mixture of polyfunctional silsesquioxane-based nanoparticles including POSS structures (POSS-M) with a small deviation of the degree of condensation of the silsesquioxane frame (narrow *n* distribution) under relatively short and simple reaction route [17]. The presence of hydroxylic and *tert*-amine groups makes the final compounds suitable for further functionalization [18,19] and usage for creation of organo-inorganic hybrids.

In the present work we report on the synthesis and results of structural studies of solid films of segmented PU–POSS polymers obtained through such polyfunctional POSS-M creation route.

## 2. Experimental section

### 2.1. Materials

3-Aminopropyl triethoxysilane (Aldrich, 98% purity) was additionally purified by distillation (b.p. 76 °C/5 mm; $n_D^{25} = 1.4200$). Glycidol (Aldrich, 96%) was used as-received. Oligo(oxypropylene glycol) (Aldrich) with a molecular weight ($M_n$) 1000 g/mol was dried under vacuum (2 torr at 90 °C); toluene diisocyanate (TDI, the mixture of 2,4- and 2,6-isomer in the ratio of 20:80, Bayer AG) and *n*-butylisocyanate (Aldrich) were purified by vacuum distillation, and dimethylformamide (DMF, Aldrich) was purified by the reaction with polyisocyanate followed by distillation under vacuum prior usage. Isocyanate prepolymer (IFP) of $M_w$ 1458 g/mol was synthesized by a reaction of oligo(oxypropylene glycol) $M_w$ 1000 g/mol with a twofold molar excess of TDI.

### 2.2. Synthesis of POSS-containing mixture (POSS-M)

Synthesis of the initial POSS-M component was carried out according to the technique described in Ref. [17]. However, in contrast to the latter, the stage of the final product purification via precipitation into acetone from methanol solution was introduced in the synthesis [19]. The OH group content in the POSS-M compounds was estimated by a reaction with an excess of *n*-butylisocyanate followed by measuring unreacted isocyanate content by a classical method described in Ref. [20]. The content of tertiary amine groups in POSS was taken into account in the analysis.

### 2.3. Synthesis of polyurethanes based on the POSS-M

PUs based on the POSS-M fragments were synthesized by a reaction of POSS-M and IFP with calculated ratios of OH/NCO equal to 5/1 (20% OH groups of POSS-M react with isocyanate), 2/1 (50% OH groups of POSS-M react with isocyanate), and 5/4 (80% OH groups of POSS-M react with isocyanate). The obtained PU–POSS copolymers contained ~6 wt.%, 2.8 wt.%, and 1.9 wt.% of the inorganic phase $(SiO_{1,5})_x$ correspondingly and have been designated as PU–POSS-6-N or PU–POSS-6-B, PU–POSS-3-N or PU–POSS-3-B, and PU–POSS-2-N or PU–POSS-2-B (where designations N and B are used to distinguish between “cross-linked”-“network” and “branched” chemical architectures of the copolymers). Details of the PU–POSS copolymer synthesis can be found below.

#### 2.3.1. PU–POSS-6-N

Solution of 1 g IFP in 0.6 ml DMF was added to a solution of 0.583 g POSS-M in 1 ml of DMF. After stirring for several seconds (to prevent gelation), the solution was cast on glass slides and kept at ambient temperature overnight and then at 60 °C until achieving a constant mass.

#### 2.3.2. PU–POSS-3-N and POSS–PU-2-N

These were prepared in a similar way (solution of 2 g IFP in 1 ml DMF was added to a solution of 0.47 g of POSS-M in 1.5 ml of DMF in the former case, and solution of 3 g of IFP in 2 ml of DMF was added to a solution of 0.437 g of POSS-M in 1.5 ml of DMF in the latter case).

#### 2.3.3. PU–POSS-6-B

The solution of 1.83 g of IFP in 10 ml of DMF was added to a solution of 1.063 g of POSS-M in 15 ml of DMF. The mixture was stirred for 8 h at 60° C until complete consumption of the isocyanate groups. After that the solution was cast on glass slides and kept at ambient temperature overnight and then at 60 °C until achieving a constant mass.

#### 2.3.4. PU–POSS-3-B and PU–POSS-2-B

These were prepared in a similar way (solution of 2.29 g of IFP in 17 ml of DMF was added to a solution of 0.503 g of POSS-M in 8 ml of DMF for the former and solution of 3.664 g of IFP in 25 ml of DMF was added to a solution of 0.518 g of POSS in 12.4 ml of DMF for the latter).

Polymer films for structural studies were prepared by casting the polymer solution on glass slides (for AFM) or Teflon substrates followed by peeling them off for X-ray diffraction experiments in a transmission mode. The thickness of the cast films on glass substrates prepared for AFM scanning was 5–6 μm while the thickness of unsupported films used for SAXS studies was (200 ± 20) μm.

### 2.4. Experimental techniques

Gel permeation chromatographic (GPC) measurements were carried out in a DMF solution using a Waters Breeze 1500 system with the application of polystyrene calibrating standards.

The structure of PU–POSS films solution-cast on glass surface has been studied with atomic force microscopic (AFM) technique. For this an Autoprobe CP (Thermomicroscopes, USA) microscope operated in a tapping mode has been employed.

Small angle X-ray scattering (SAXS) studies have been carried out with a vacuum Kratky camera. Copper anode tube (Cu Kα line) radiation monochromated with total internal reflection and nickel filters has been used [21]. Data collection has been carried out in a regime of multiple step scanning of a scintillation detector in the range of scattering angles 0.03°–4.0°, which corresponded to the values of wave vectors $q$ of 0.022–2.86 $\text{nm}^{-1}$ ($q = 4\pi \sin\theta/\lambda$, where $\theta$ is the half of the diffraction angle $2\theta$, and $\lambda$ is the wavelength of X-ray radiation emitted by the copper anode $\lambda = 0.154$ nm). SAXS method is sensitive to local variations of the density due to the presence of domains of higher than average density or voids with smaller than average density and distribution of such heterogeneity with characteristic dimensions (determined as $2\pi/q$) in the range of 2–280 nm. The initial treatment of the data has been performed with an FFSAXS program [22]. It included the procedures of background noise subtraction, normalizing of the diffraction curves to absolute values of scattering, and application of collimation corrections. The treated diffraction curves were used for calculations of a mean square fluctuation of the electron density and three-dimensional correlation functions in accordance to the procedures described in Ref. [23].

## 3. Results and discussion

Chemical synthesis of POSS-M system is based on a reaction of hydrolytic condensation of the product of interaction of 3-aminopropyl triethoxysilane with a twofold molar excess of glycidol (Scheme 1) [17–19].

The main peculiarity of the process is high homogeneity of the reactive system as the initial substances and all the intermediate and final products have good solubility both in water and in the methanol solvent. The final product is glassy-like, optically transparent, hygroscopic and soluble in water, methanol, DMF, and dimethylsulfoxide (DMSO) but not soluble in acetone, dioxane, benzene, toluene, and pyridine. Under heating to or above 60 °C it becomes soft and obtain fluidity.

The final product is a mixture of nanoparticles with dimensions ~3 nm in accordance to Ref. [17]. Application of matrix assisted laser desorption/ionization time-of-flight (MALDI-TOF) mass spectrometry technique [17] has revealed that this mixture contained hydroxyl- and amino-containing silsesquioxanes characterized with a variety of structures: open structures with at least five silanol groups in molecules, ladder type structures (with four silanol groups per molecule), partially condensed polyhedral structures with the number of silanol groups per oligomer from 1–3, and fully condensed POSS moieties. Presence of a big number of hydroxylic groups in POSS-M structures as well as aliphatic *tert*-amine groups makes these compounds very attractive for synthesis of nanostructured OIH of the polyurethane type.

In accordance to GPC results these products are characterized with a polymodal molecular mass distribution with an average polydispersity index of 1.11. The number average molecular mass $M_n =$ 4040 g/mol corresponds to an empirical formula of the oligosilsesquioxane: $[(HOCH_2CH(OH)CH_2)_2N(CH_2)_3SiO_{1,5}]_x$, with $x$ value ~16.

As has been mentioned above, POSS-M is a mixture of polyfunctional compounds of different chemical architecture including polyhedral compounds having tertiary amines and around 50 hydroxylic primary and secondary end groups in the organic shell. As a result of such polyfunctionality of POSS-M, one should expect formation of a gel phase at a very early stage of its reaction with IFP. Formation of a network structure has been really observed for the first set of samples (PU–POSS-6-N, PU–POSS-3-N and PU–POSS-2-N) when polymer concentration in DMF solution was 50% independent of the NCO/OH ratio. Therefore, immediately after mixing the components and vigorous stirring polymer solutions were cast on a solid substrate to avoid gelation of the solution. The formation of a network structure could then happen in the cast polymer film. Solution-cast polymer films were optically transparent and insoluble in DMF and DMSO. In case when polymer solution concentration in DMF has been reduced to 10% or lower, the gelation process has not been observed under similar preparation conditions and the same NCO/OH ratio even under complete consumption of NCO groups (samples PU–POSS-6-B, PU–POSS-3-B and PU–POSS-2-B). Special additional experiments demonstrated that the content of the NCO groups in IFP remained unchanged during the duration of the reaction (i.e., 8–10 h at 60 °C) under the same concentration of the polymer in DMF solution if the POSS fragments were not present in the reaction mixture. These observations confirmed that the reaction between NCO and OH groups happened primarily during the process of PU–POSS synthesis and there was practically no by-side reaction, which could involve participation of the NCO groups. The obtained, in such chemical process, films preserved their solubility in DMF with an exception of PU–POSS-6-B sample, which was soluble in DMSO only. Obviously, branched POSS-M containing PUs were formed under the specified conditions.

Synthesis of the POSS-M containing PU with a variable number of hydroxylic groups in the final product can be represented by a general reaction shown in Scheme 2, and has been accomplished through reaction of POSS-M with IFP carried under various ratios of OH to NCO groups.

In such a way, PU–POSS copolymers with a different content of hydroxyl and urethane fragments (different OH/NCO ratio) in the PU portion (see Section 2) have been synthesized.

Chromatograms of the polyurethanes PU–POSS-6-B and PU–POSS-3-B are polymodal in their nature with the average values of molecular masses and polydispersity indices: $M_n = 17{,}090$ g/mol, $M_w/M_n = 1.97$ (POSS–PU-6B) and $M_n = 19{,}163$ g/mol, $M_w/M_n = 2.34$ (POSS–PU-3B).

Infrared (IR) spectra of the both synthesized sets (cross-linked and branched) are identical (Fig. 1). They are characterized with a broad absorption band with the maximum near 3400 cm$^{-1}$ typical for stretching vibrations of OH and N–H groups of PUs. Stretching vibration band of C=O group of the urethane fragments of cross-linked polymers is located at 1727 cm$^{-1}$ (PU–POSS-6-N), 1721 cm$^{-1}$ (PU–POSS-3-N) and 1716 cm$^{-1}$ (PU–POSS-2-N), while

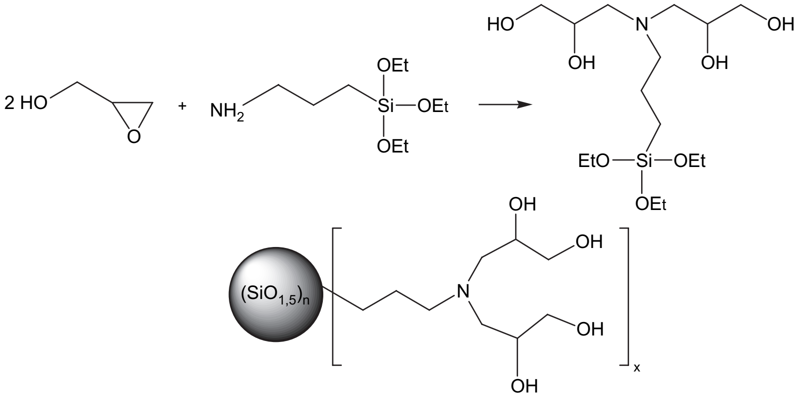

Scheme 1.

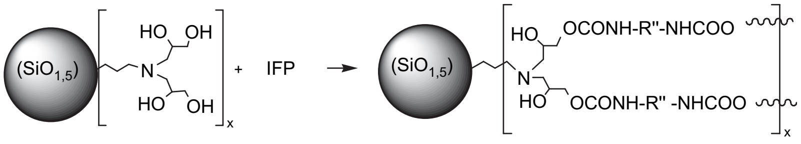

R'' $=$R-NHCOO(R'O)$_{18}$-CONH-R
R $=$ 2,4-,2,6-$C_6H_3(CH_3)$; R' $=$ $CH_2CH(CH_3)$

**Scheme 2.**

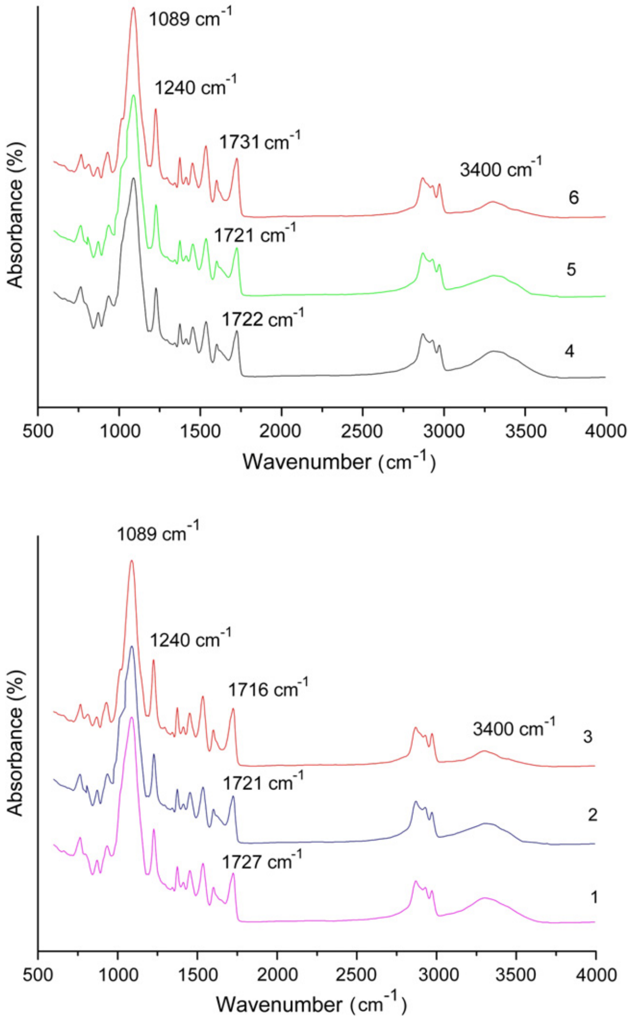

**Fig. 1.** Infrared absorption spectra of PU–POSS-6-N (1), PU–POSS-3-N (2), PU–POSS-2-N (3), PU–POSS-6-B (4), PU–POSS-3-B (5), and PU–POSS-2-B.

polymers with the branched architecture have different peak positions: 1722 $cm^{-1}$ (PU–POSS-6-B), 1721 $cm^{-1}$ (PU–POSS-3-B) and 1731 $cm^{-1}$ (PU–POSS-2-B). C=O vibrations of urea or isocyanurate groups do not appear in the IR spectra. The vibration band in the range of wavelengths 1000–1180 $cm^{-1}$ corresponds to stretching vibrations of Si–O–Si bonds. The vibration band of Si–$CH_2$ groups is observed at 1240–1280 $cm^{-1}$.

Complex several-level hierarchy of the structural organization of the POSS-M containing PUs could be recognized from both X-ray diffraction and AFM studies. Fig. 2 shows the most representative features of the PU–POSS morphology. All the samples are very smooth with the root mean square (RMS) roughness in the range of 0.4–1.6 nm when measured for $1 \times 1\ \mu m^2$ to $5 \times 5\ \mu m^2$ regions of the AFM topography images, while increasing to 3–8 nm for larger scales. As follows from the AFM images, heterogeneity of the PU–POSS surface topography is generally reduced with the reduction of the POSS-M content. The morphology of all samples is represented with nanometer size particles (2–3 nm in diameter) or their agglomerates of 20–30 nm average sizes. POSS particles are coated with a thin (skin) layer of the organic (polymer) phase, which makes the composites' surface visually smooth. The branched samples are characterized with more developed porous structure in comparison to the cross-linked ones. RMS roughness measured for $2 \times 2\ \mu m^2$ regions is decreasing when concentration of the POSS-M component is going down: 1.5 nm for PU–POSS-6-B, 0.6 nm for PU–POSS-3-B, and 0.4 nm for PU–POSS-2-B samples. For the cross-linked samples (the bottom row in Fig. 1) this trend is not so well pronounced: RMS = 0.8 nm for both PU–POSS-6-N and PU–POSS-3-N compositions and 0.4 nm for PU–POSS-2-N sample. This is probably due to the fact that the morphology of cross-linked samples is determined by both physical and chemical structural factors (i.e., by POSS content and density of the polymer network).

Some of PU–POSS samples under study experienced shrinkage in the process of solution-cast film drying, which caused formation of microscale heterogeneities ("valleys") of several micrometers in size. The effect is observed for cross-linked samples and can be understood as a nonuniform densification as a result of simultaneous evaporation of the solvent and formation of the network structure in the process of film formation. Local gradients of the density developed during fast evaporation of the solvent lead to development of local stresses and formation of cracks in some places. On the contrary, more uniform shrinkage resulting in a smooth surface without cracks has been observed for the branched PU–POSS samples. One of the above-discussed valleys is shown in Fig. 3. Interestingly, the surface structure observed for the bottom of the valley was different in comparison with the average surface topography. As can be observed from Fig. 3, several individual nanoparticles with the size 2–3 nm are clearly seen in the valley region while only conglomerates of such particles can be registered for the top surface of the polymer film. One should note that visible lateral dimensions of the particles are a result of the mathematical procedure of convolution of the AFM tip shape and the particles' shape and therefore cannot be used for the particles' actual size estimation without exact knowledge of the tip shape. On the other hand, the height of these nanometer scale "undulations" can be used as a direct measure of the nanoparticles' size.

SAXS experiments revealed that processes of microphase segregation and formation of nano-sized domains enriched with the inorganic phase (POSS-M fragments) take place during synthesis of the PU–POSS hybrids under study. Fig. 4 shows dependence of a logarithm of scattered X-ray intensity on the wave vector $q$. One can see that the scattering curve of the branched POSS–PU-6B sample is characterized with a well pronounced maximum corresponding to the wave vector 0.42 $nm^{-1}$, which is a signature of spatial periodicity of 15 nm. On the other hand, the network POSS-M containing PU of the same composition has similar maximum with much weaker intensity. Moreover, this maximum is smeared and shifted towards a higher value of the wave vector $\sim$0.64 $nm^{-1}$ (which corresponds to periodicity of 9.7 nm).

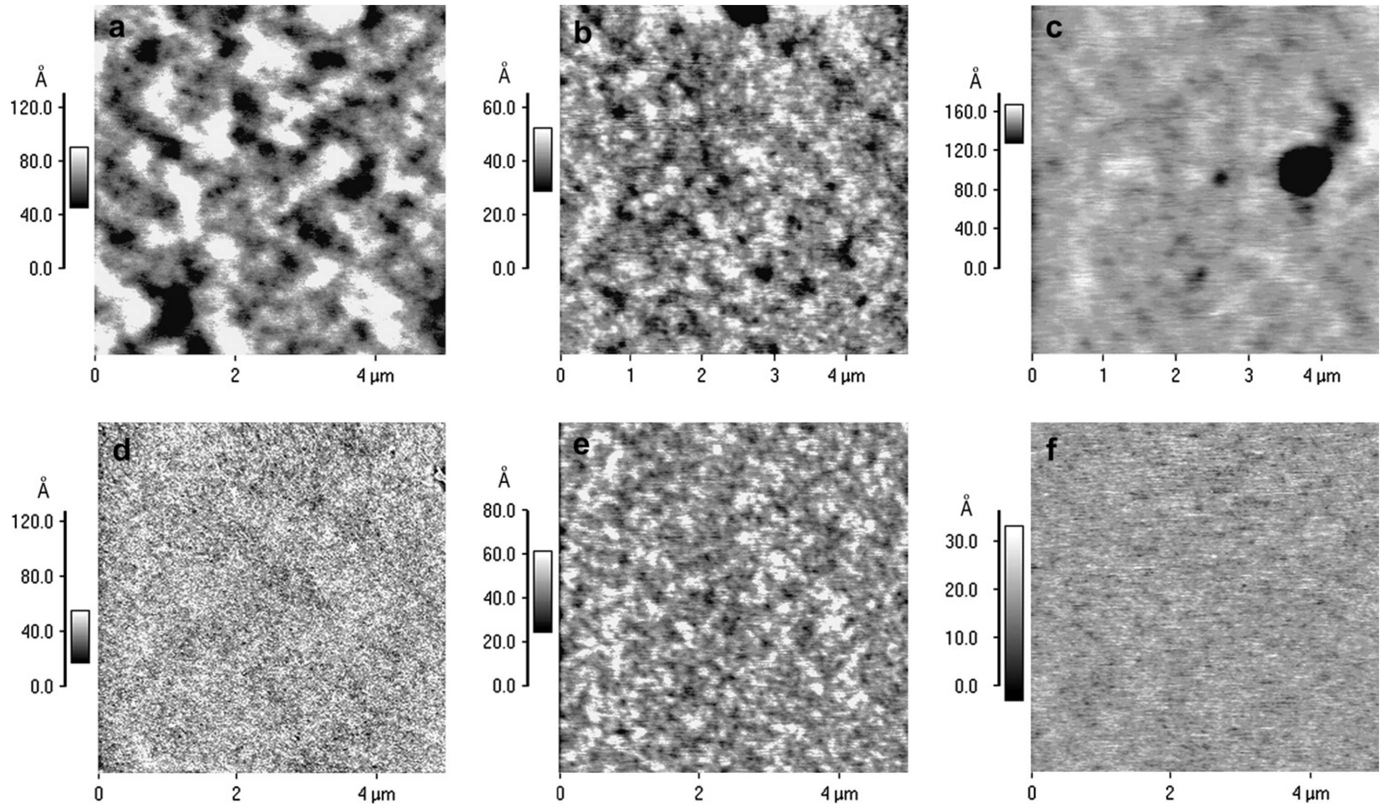

**Fig. 2.** AFM topography images of branched PU–POSS-6-B (a), PU–POSS-3-B (b), PU–POSS-2-B (c), and cross-linked PU–POSS-6-N (d), PU–POSS-3-N (e), PU–POSS-2-N (f) films.

The appearance of a small angle maximum on the diffraction curves is generally interpreted as a feature of a microphase separation in the system with formation of nano-sized regions enriched with one of the components (inorganic fragments of the polymer chains in our case). These nano-sized regions (nanoclusters) form a paracrystalline (imperfect) lattice in the volume of the polymer sample, which is responsible for the observed X-ray scattering peaks [24].

Possibility of ordered crystalline structure formation was previously reported for both functionalized POSS molecules [25] and polymer-POSS systems [9,10,26]. Formation of ordered clusters of POSS units within a polymer matrix was also confirmed with computer simulations [27]. In the latter case formation of clusters with the average size of 2–3 nm and a radial distribution function with sharp peaks corresponding to average distances less than 1.5 nm (the maximum distance between silicon atoms within nearest neighbor POSS moieties) were demonstrated when the system was cooled down from 500 K (disordered state) to 300 K (ordered state). The calculated radial distribution function of POSS positions pointed out a long-range correlation in the POSS units' positions spreading beyond the values typical for amorphous materials and suggesting organization of the neighboring POSS particles into more ordered structural arrangement typically observed for a crystalline phase. These simulations can be considered, therefore, as a theoretical prediction for possible paracrystalline packaging in the system.

Calculated from the curves shown in Fig. 4 values of the mean square fluctuations of the electron density are $0.234 \times 10^{-2}$ (mol el)$^2$/cm$^6$ and $0.192 \times 10^{-2}$ (mol el)$^2$/cm$^6$ for the branched and cross-linked POSS-M containing PU, respectively. These values of the electron density can be used for the estimation of the degree of microphase separation in the system as discussed later.

Fig. 5 shows a result of diffuse background subtraction from the experimental X-ray diffraction curves. The background was approximated with an exponential function, which is typical for amorphous and semi-crystalline polymers [21]. Analysis of the obtained curves revealed their Gaussian shape, which gives evidence of a normal distribution of the centers of mass of scattering elements in space. Gaussian distribution is a signature of either polydispersity of spherical scattering centers or a spatial inhomogeniety in orientation of ellipsoidal scattering centers of exactly the same size and shape. The latter explanation looks very unlikely considering MALDI-TOF data for the POSS units [17], while the former looks realistic and is in tune with our expectations based on the polydispersity of the POSS-M nano-fragments. A transition from branched to cross-linked POSS-M containing PU leads to a significant reduction of the integral intensity of corresponding maxima. Simultaneously the full-width at half-maximum (FWHM) value is larger for the cross-linked POSS-M containing PU (0.43 nm$^{-1}$) in comparison to a 0.26 nm$^{-1}$ value for the branched sample. These results demonstrate the general trend for reduction of the fraction of ordered material and increasing defectness of the paracrystalline order due to increased topological complexity of the cross-linking system.

Fig. 6 shows the results of further analysis of the X-ray curves through calculating of the three-dimensional correlation functions. The correlation curves are characterized with the first order maxima only. The position of the first maximum corresponds to an average distance between neighboring nano-sized heterogeneity regions ($r$) and can be estimated as 17.5 nm and 11 nm for the branched PU–POSS and cross-linked PU–POSS sample, respectively. Comparison of the interplanar distances $D$ found from the positions of the maximum of the corresponding scattering curve (Figs. 4 and 5) with the values of $r$ gives the average $D/r$ ratio in the range of 1.13 to 1.16. Such values are typical for a hexagonal symmetry in

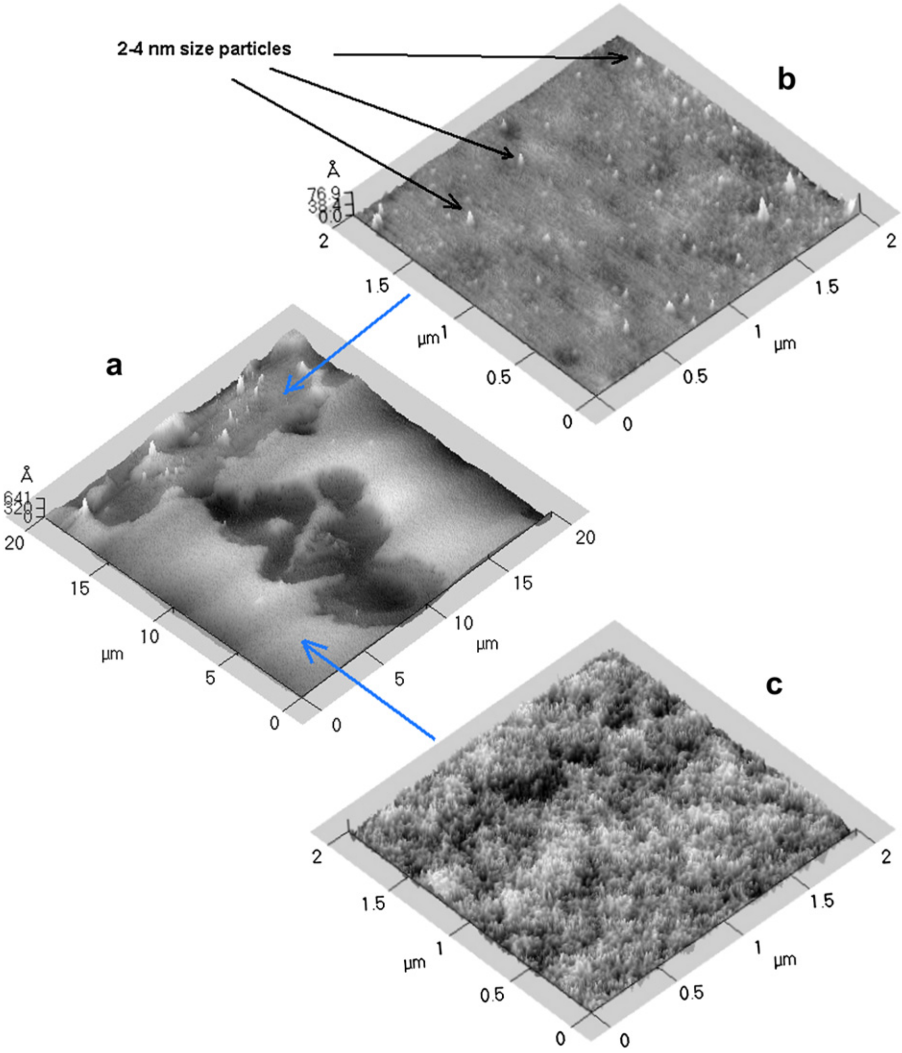

**Fig. 3.** AFM topography images of the surface of PU–POSS-6-N film after drying (a) and two characteristic types of the surface structures observed for cracks (b) and the top of the film regions (c).

packaging of the scattering units within the paracrystalline macrolattice [23]. An alternative closely packed paracrystalline structure to be considered would possess a cubic symmetry. However, in the case of cubic paracrystalline lattice the average distance between neighboring heterogeneity regions would be approximately the same as the interplanar distance (i.e., $D/r \approx 1$), which is not observed in our SAXS results.

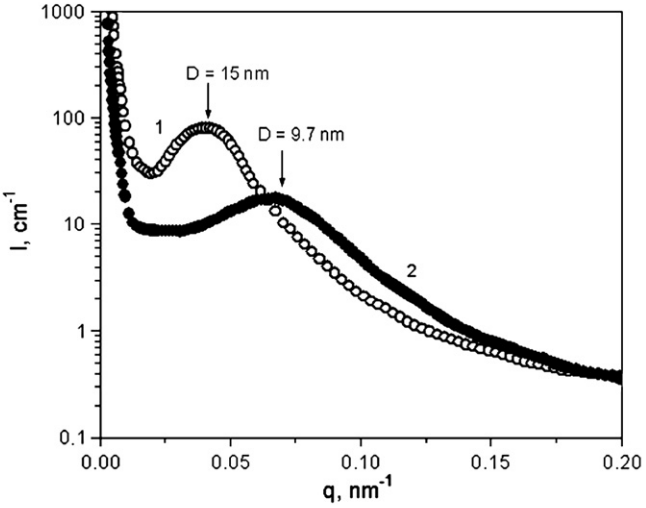

**Fig. 4.** Semi-logarithmic scale representation of experimentally measured small angle X-ray diffractograms for PU–POSS-6-B (curve 1) and PU–POSS-6-N (curve 2).

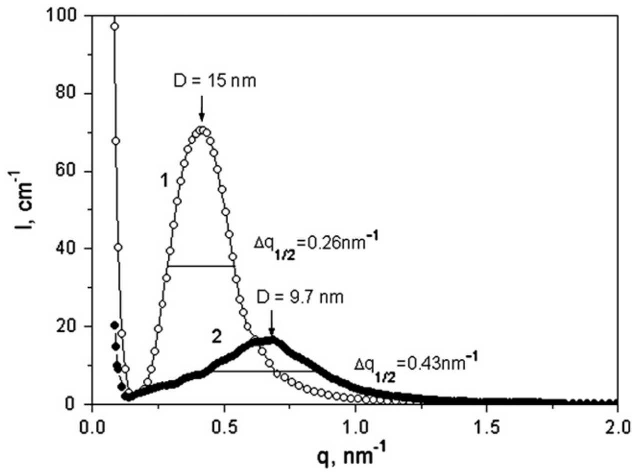

**Fig. 5.** X-ray scattering curves after background intensity subtraction PU–POSS-6-B (curve 1) and PU–POSS-6-N (curve 2).

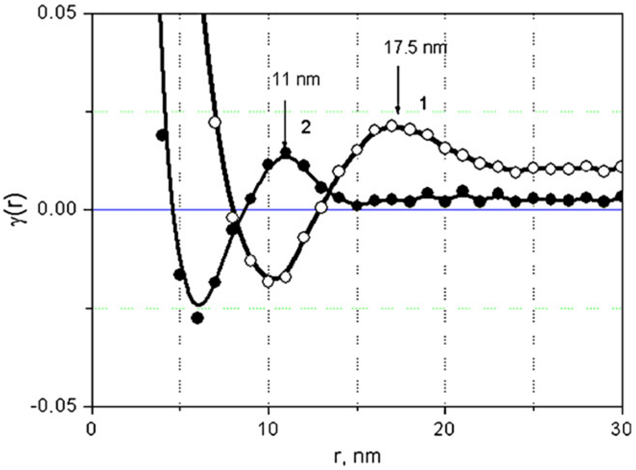

**Fig. 6.** 3D autocorrelation functions calculated from SAXS data for PU–POSS-6-B (curve 1) and PU–POSS-6-N (curve 2) samples.

One more interesting parameter, which can be estimated from the SAXS data presented in Fig. 6, is the position of the first minimum on the three-dimensional correlation functions. This parameter puts an upper limit for the possible size of the periodically arranged nano-sized regions. Consideration of the curves in Fig. 6 allows conclusion that these values are 6 nm and 10 nm for the cross-linked and branched copolymers under study, respectively. Therefore, the diameters of these structural elements cannot exceed 12 nm for PU–POSS-6-N and 20 nm for PU–POSS-6-B samples.

Estimation of the average size of nano-heterogeneous regions has been performed with consideration of their volume fraction (~4 vol.%). We have used the value of the density of the inorganic core (POSS structure with average composition $SiO_{1.5}$, $\rho = 1.8$ g/cm$^3$) in such calculations. For the cross-linked polymer with the value of spatial periodicity of nano-sized clusters $D = 9.7$ nm and with the assumption of their perfect spherical shape, one can calculate the size of nano-heterogeneous regions to be 4.1 nm, while in the case of hyperbranched polymer ($D = 15$ nm) the size of the inorganic POSS-enriched core is higher (6.4 nm). The estimated core size corresponds to several POSS-M units and suggests their aggregation into clusters [17]. One should notice that these structural parameters agree with estimations based on three-dimensional correlation function analysis. For illustration purpose PU–POSS material with approximately 6 wt.% (or 4 vol.%), of inorganic phase was used. The degree of microphase separation has been found from comparison of the experimental mean square fluctuations of the electron density with the theoretical value obtained in consideration of the bulk densities of the components and their volume fractions in the system [24]. The value of the mean square fluctuation of the electron density was found to be $0.353 \times 10^{-2}$ (mol el)$^2$/cm$^6$, which leads to the calculated (theoretical) values of the degree of components' segregation of 66% and 54% for the branched and cross-linked POSS-M containing PUs correspondingly. These values can be considered as approximation of a fraction of the inorganic phase in the nano-heterogeneous regions.

Structural organization of considered PU–POSS systems at different structural levels revealed by our AFM and SAXS studies is schematically presented in Fig. 7. The basic nanoscale unit of the structure is an inorganic core POSS moiety coated with organic PU shell. Phase segregation in the system leads to the formation of small aggregates of such units at the next "mesoscopic level" of the structure. Again, such clusters or aggregates have the inner inorganic core surrounded by polymer "hair". Both individual PU–POSS units and their aggregates can be observed with AFM technique. On the next level of the structural organization the PU–POSS clusters form nanoscale domains with the paracrystalline order of inorganic core units inside of a polymer matrix formed by interpenetrating macrochains in case of branched systems or polymer network in case of the cross-linked ones. The existence of such domains is revealed by the AFM, while their average size can be confirmed by both direct microscopic observation and analysis of the SAXS curves (the width of small angle peaks and correlation function analysis). The internal paracrystalline order of the domains could be revealed from SAXS diffraction curves as discussed above. Finally, the domains form a "micro-structural level" of organization with a porous surface (spaces between domains) in case of branched PU–POSS and monolithic matrix in case of the cross-linked systems. This level of structural organization could be easily accessed with the AFM observations.

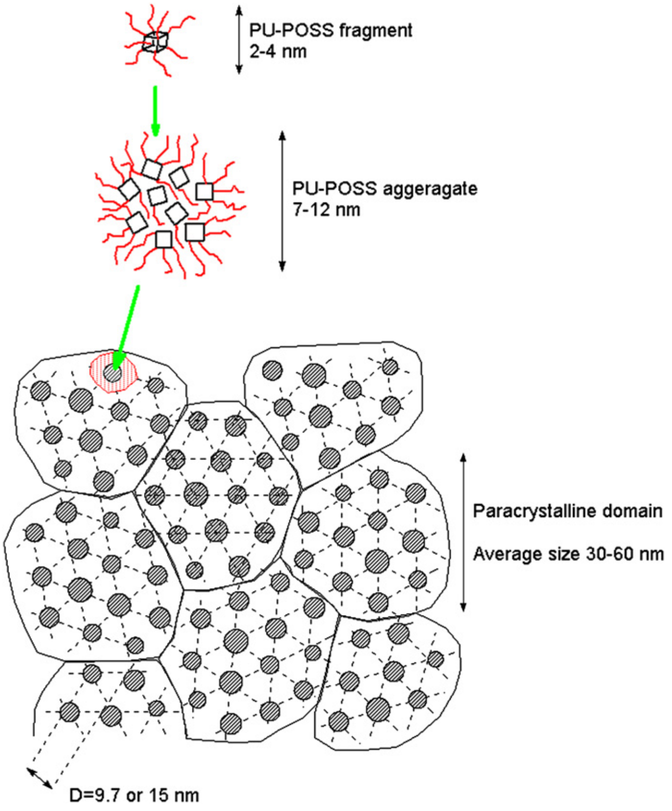

**Fig. 7.** Multi-level structural organization of PU–POSS systems revealed in AFM and SAXS experiments.

## 4. Conclusions

We have demonstrated that processes of microphase segregation and formation of nano-sized clusters enriched with the inorganic phase (POSS-M fragments) take place during synthesis of the hybrid organic–inorganic POSS-M containing PUs under study. These nano-heterogeneity regions contain ~66 vol.% of $SiO_{1.5}$ and form a paracrystalline lattice with hexagonal symmetry and characteristic interplanar periodicity of around 15 nm, which can be detected with small angle X-ray scattering and visualized with atomic force microscopy. Simultaneously the average size of the smallest inorganic phase nano-inclusions can be estimated as 2–3 nm, which corresponds to several POSS cages in size.

Cross-linked POSS-M containing PUs as topologically more complex systems are characterized with a diffusion-limited microphase segregation process. Nano-heterogeneity regions are therefore smaller in size, have smaller content of the inorganic phase

(~54 vol.%) and form a less perfect paracrystalline order with the periodicity of 9.7 nm in this case.

A complex several-level hierarchy of the structural organization of POSS-M containing PUs can be recognized from both X-ray diffraction and AFM experiments. The AFM images demonstrate poorer ordering of the paracrystalline structure due to generally higher disorder of the surface in comparison to the bulk state of the polymer systems.

## References

[1] Koberstein JT, Galambos AF, Leung LM. Macromolecules 1992;25:6195–204.
[2] Koberstein JT, Leung LM. Macromolecules 1992;25:6205–13.
[3] Kickelbick G. Prog Polym Sci 2003;28:83–114.
[4] Baney RH, Ito M, Sakakibaro A, Suzuki T. Chem Rev 1995;95:1409–30.
[5] Kim BS, Mather PT. Macromolecules 2002;35:8378–84.
[6] Kim BS, Mather PT. Polymer 2006;47:6202–7.
[7] Dvornic PR, Hartmann-Thompson C, Keinath SE, Hill EJ. Macromolecules 2004;37:7818–31.
[8] Fu BX, Zhang W, Hsiao BS, Rafailovich M, Sokolov J, Johansson G, et al. High Perform Polym 2000;12:565–71.
[9] Fu BX, Hsiao BS, White H, Rafailovich M, Mather PT, Leon HG, et al. Polym Int 2000;49:437–40.
[10] Fu BX, Hsiao BS, Pagola S, Stephens P, White H, Rafailovich M, et al. Polymer 2001;42:599–611.
[11] Wu J, Ge Q, Burke KA, Mather PT. Mater Res Soc Symp Proc 2005;847: P.EE10.2.1.
[12] Turri S, Levi M. Macromolecules 2005;38:5569–74.
[13] Nanda AK, Wicks DA, Madbouly SA, Otaigbe JU. Macromolecules 2006;39: 7037–43.
[14] Oaten M, Choudhury NR. Macromolecules 2005;38:6392–401.
[15] Neumann D, Fisher M, Tran L, Matisons JG. J Am Chem Soc 2002;124:13998–9.
[16] Liu H, Zheng S. Macromol Rapid Commun 2005;26:196–200.
[17] Mori H, Lanzendörfer MG, Müller AHE, Klee JE. Macromolecules 2004;37: 5228–38.
[18] Muthukrishnan S, Plamper F, Mori H, Müller AHE. Macromolecules 2005;38: 10631–42.
[19] Tereshchenko TA, Shevchuk AV, Shevchenko VV, Snegir SV, Pokrovskii VA. Polym Sci Ser A 2006;48:1248–56.
[20] Dombrow BA. Polyurethanes. New York: Reinhold Publishing Corporation; 1957.
[21] Lipatov YS, Shilov VV, Gomza YP, Kruglyak HE. X-ray diffraction techniques for study of polymer systems. Kiev: Naukova Dumka; 1982 [in Russian].
[22] Vonk CG. J Appl Crystallogr 1974;8:340–1.
[23] Hosemann R, Bagchi SN. Direct analysis of diffraction by matter. Amsterdam: North Holland Co; 1962.
[24] Bonart R, Müller EH. J Macromol Sci Phys B 1974;10:177–89.
[25] Waddon AJ, Coughlin EB. Chem Mater 2003;15:4555–61.
[26] Zheng L, Waddon AJ, Farris RJ, Coughlin EB. Macromolecules 2002;35:2375–9.
[27] Capaldi FM, Rutledge GC, Boyce MC. Macromolecules 2005;38:6700–9.